

Toward VCSEL-Based Integrated Optical Traps for Biomedical Applications

Andrea Kroner

A new concept to miniaturise optical trapping and manipulation systems is presented. Integrated optical traps based on top-emitting vertical-cavity surface-emitting lasers (VCSELs) with near-infrared emission in combination with photoresist microlenses were fabricated, characterised and demonstrated. Elevation and trapping of $10\mu\text{m}$ -sized polystyrene particles in water is achieved at optical output powers as small as 9mW .

1. Introduction

The possibility to trap and manipulate micrometer-sized particles by a laser beam was demonstrated for the first time in 1970 [1]. The effect is based on the momentum conservation of photons which are reflected and refracted when hitting a transparent spherical object. Considering a parallel laser beam the interaction leads to the so called scattering force, which pushes the particle forward, parallel to the incident beam. However, if the beam shows an additional transverse intensity gradient, also a force component in the transverse direction is present. Figure 1 illustrates the occurrence of this so-called transverse gradient force with a ray-optical model. When a ray is refracted by a sphere, the associated momentum change of the photons results in an outward oriented force on the particle. If the incident intensity is higher on one side of the sphere, the particle experiences a total force toward the intensity maximum. There the particle remains fixed in the transverse direction due to a vanishing net transverse force. A two-dimensional optical trap is thus established. By tightly focussing a laser beam, even three-dimensional optical trapping can be achieved due to the strong longitudinal intensity gradient and the resulting longitudinal gradient force.

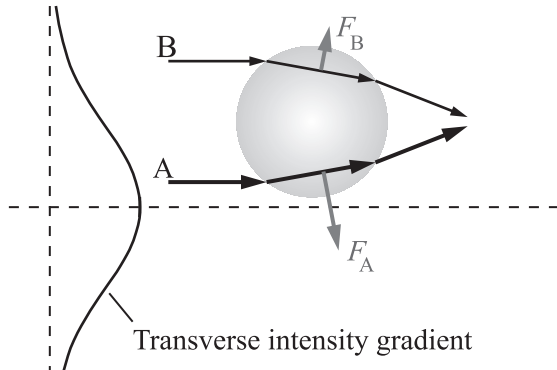


Fig. 1: Origin of the transverse gradient force caused by a parallel laser beam with a transverse intensity gradient. The refraction of the rays A and B leads to the forces F_A and F_B on the particle. Since ray A is stronger than ray B, the net force points toward the intensity maximum.

In recent years, optical trapping has gained increasing attention, especially in the field of biophotonics. Here, the possibility of contact-free optical manipulation of biological material like DNA or cells with forces in the pN range was exploited in mechanical and spectral studies [2] as well as transport and sorting applications [3]. More recently, the use of VCSELs as laser sources in optical trapping systems has attracted particular interest since they are much smaller and less expensive than commonly used Nd:YAG lasers and, unlike edge-emitting laser diodes, require no additional beam corrections. A further advantage of VCSELs is the easy fabrication of monolithic two-dimensional laser arrays, permitting a straightforward implementation of multiple optical traps. VCSEL arrays originally designed for optical communications were used to trap several yeast cells individually at the same time [4], to translate DNA bound to microbeads non-mechanically between traps [5] or to stack polystyrene microspheres [6]. To achieve stable three-dimensional trapping by a tightly focussed laser beam, a high numerical aperture objective was used in all experiments, requiring a comparatively bulky optical setup. In this contribution we present a new concept to reduce the geometrical dimensions by integrating microlenses directly on the laser output facet. With this setup, referred to as integrated optical trap, highly compact two-dimensional optical trapping is achieved.

2. Setup

Figure 2 shows a schematic of the integrated optical trap setup. The system is based on GaAs/AlGaAs top-emitting VCSELs grown by molecular beam epitaxy, with emission wavelengths in the 850 nm range. For current supply a ring contact is placed on top of the upper p-doped Bragg-mirror. The active diameter of the laser is defined by selective oxidation. To focus the VCSEL output beam to a beam waist of some micrometers in diameter, a photoresist microlens is integrated on the output facet, partially covering the contact metallisation. The sample stage, containing the particles to be manipulated, consists of a cover slip and an only 30 μm thick glass substrate, separated by a 50 μm thick polydimethylsiloxane (PDMS) spacer. The stage is placed close to the laser surface at a distance of about 10 μm such that the beam waist of the focussed laser beam is located just above the lower glass substrate.

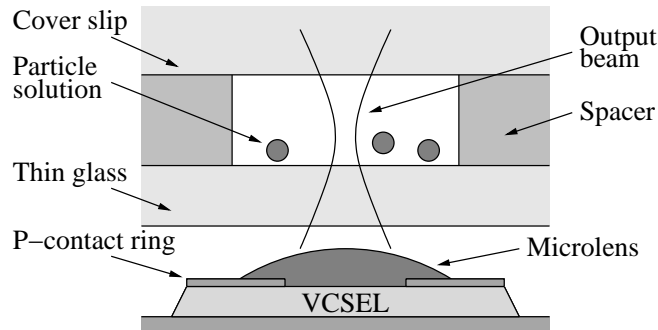


Fig. 2: Schematic of the integrated optical trap setup. The output beam is focussed by a PMGI microlens to manipulate the particles in solution. The liquid is sandwiched between a 30 μm thick glass substrate and a cover slip, which are separated by a 50 μm PMDS spacer.

3. Device Fabrication and Characterisation

After standard VCSEL processing, the microlens consisting of polymethylglutarimide (PMGI) photoresist is fabricated on top of the laser output facet. PMGI is a suitable material for microlenses due to its transparency in the near-infrared spectral region and its high thermal stability compared to other resists. By applying lithographic techniques, small resist islands are placed on top of the lasers, which assume a spherical shape during a thermal reflow process at temperatures above 250°C. The radius of curvature of the resulting lens is pre-defined by the diameter and thickness of the initial resist island. Depending on the active diameter of the laser, here ranging from 11 to 14 μm , radii of curvature of 20 to 25 μm must be realised in order to achieve the desired beam diameter at the focal point. The inset of Fig. 3 presents an optical microscope image of a completed device, showing the laser mesa with the p-contact ring and the integrated microlens. The lenses were characterised by measuring their surface profile with an atomic force microscope (AFM). The dots in Fig. 3 indicate the AFM data while the solid line shows a spherical fit, revealing a nearly ideal spherical shape with a radius of curvature of about 22 μm .

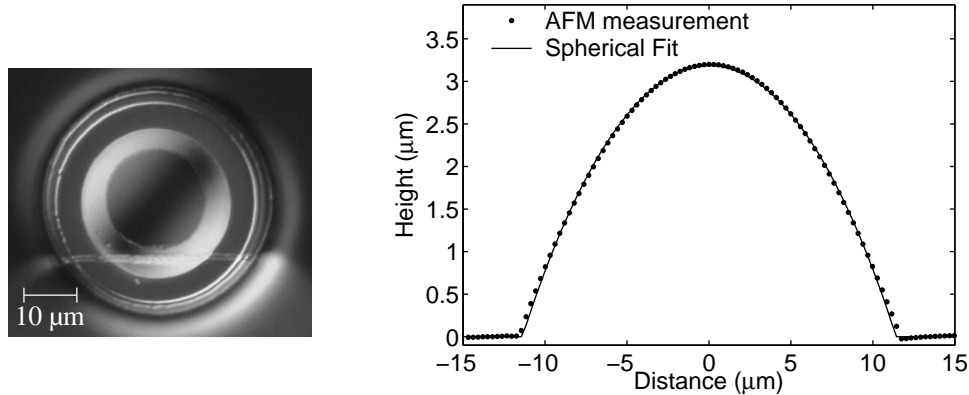


Fig. 3: Microscope image (left) and AFM height profile measurement (right) of a lensed VCSEL. The spherical fit of the AFM data shows a nearly ideal spherical shape of the lens with a radius of curvature of about 22 μm .

In Fig. 4 the operating characteristics of the same device are shown before and after the microlens was placed on its output facet. A small increase of the threshold current as well as of the differential quantum efficiency and the maximum output power is observed, which is caused by the decrease of the upper mirror reflectivity by the microlens material. An optical output power of up to 17 mW is available from this device. The VCSEL has an active diameter of 13.5 μm and shows transverse multimode emission from threshold to thermal rollover with an emission wavelength of about 860 nm.

To confirm the focussing effect of the microlens, the transverse output beam profiles at different distances from the laser surface were measured by scanning the laser beam with a lensed fiber moved by piezo actuators. Figure 5 shows the scanned beam profile at distances from about 0 to 50 μm to the laser surface. A minimum beam diameter of

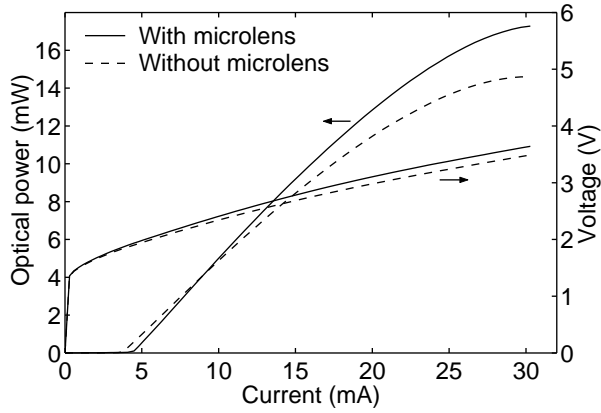


Fig. 4: Light-current-voltage characteristics of a $13.5\text{ }\mu\text{m}$ oxide aperture VCSEL with and without integrated microlens. The increase of threshold current and optical output power is explained by a reduction of the top mirror reflectivity.

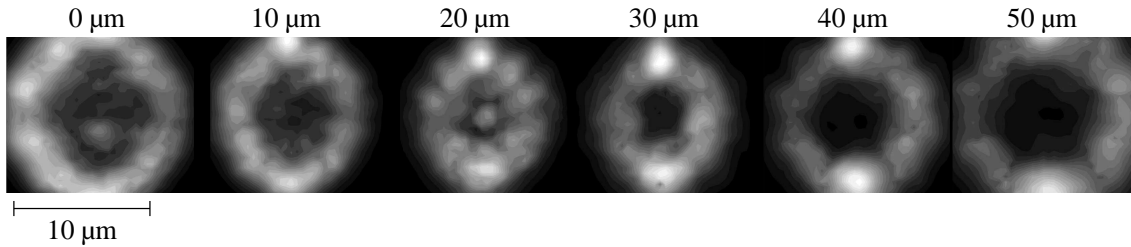


Fig. 5: Measurement of the beam profiles of a lensed device at a current of 6 mA at various distances to the laser surface, ranging from about 0 to $50\text{ }\mu\text{m}$. The focal point with a beam diameter of about $15\text{ }\mu\text{m}$ and a FWHM of $10\text{ }\mu\text{m}$ is found at a distance of 20 to $30\text{ }\mu\text{m}$.

about $15\text{ }\mu\text{m}$ and a full-width-at-half-maximum (FWHM) of $10\text{ }\mu\text{m}$, respectively, at a distance of about 20 to $30\text{ }\mu\text{m}$ (in air) are measured. In contrast, a nominally identical device without lens on the same wafer shows a continuously diverging beam. However, due to multimode emission, both laser types have a doughnut-shaped intensity profile.

4. Results

To examine the suitability of the components in optical trapping applications, the above described device was introduced in the setup shown in Fig. 2. To observe the experiments, an imaging system, mainly consisting of a CCD camera and filters, was placed above the sample stage. The experiments were performed with $10\text{ }\mu\text{m}$ -sized polystyrene particles in water since their physical properties like density and refractive index are comparable with those of biological cells.

Figure 6 shows a typical experimental sequence by means of pictures taken by the CCD camera (top view). For better comparison, corresponding schematic side views are added. Initially the particles are located at the bottom of the sample stage and drift randomly through the liquid (Figs. 6a and 6b). This drift is induced by a constant evaporation of liquid from the sample stage and was not found to be influenced by the emission state of the laser. In the present case the VCSEL emits 9 mW optical output power. When approaching the laser beam, the particle is pulled toward an intensity maximum by the transverse gradient force (Figs. 6c and 6d). Since the laser beam is only mildly focussed,

the longitudinal gradient force is not strong enough to overcome the forward scattering force which arises mainly due to reflection of photons at the particle surface. Therefore, the particle is lifted by the laser beam until it reaches the upper cover slip where it remains trapped. The elevation is observable in Figs. 6d and 6e by a blurring of the particle as it moves out of the imaging focus. In Fig. 6f, the focal point of the imaging system is adjusted to show the particle immobilised at the top of the sample stage. When the laser is turned off, it floats back to the bottom. At lower output power deflection and elevation of the particles is still observed while stable trapping at the upper cover slip is no longer achieved. Consistent results for manipulation and trapping were obtained for similar VCSELs. However, a displacement of the trapped particle with respect to the device centre is generally observed, much likely caused by the doughnut-shaped beam profile. To improve the beam quality of the VCSELs, surface relief techniques [7] will be applied as a next step.

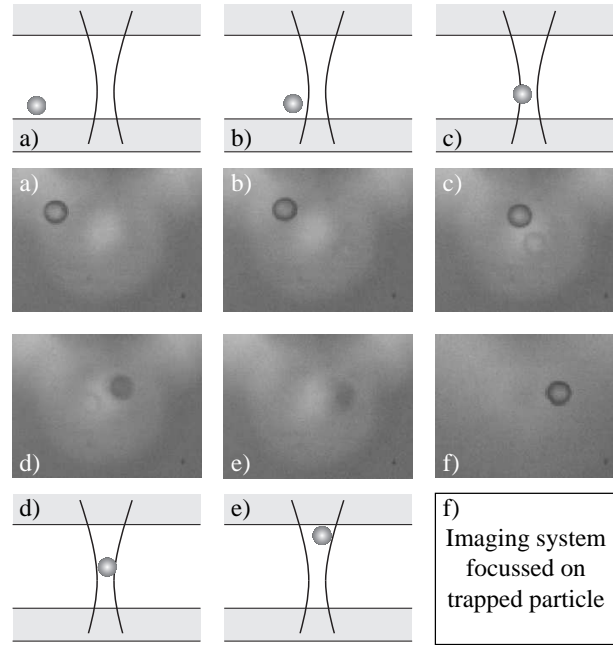


Fig. 6: Sequence of a typical trapping experiment with the integrated optical trap using a $10\ \mu\text{m}$ diameter polystyrene microsphere. For better understanding, top views by the CCD camera as well as associated schematic side views are shown. The approaching particle (a, b) is pulled toward the intensity maximum of the laser beam by the gradient force (c, d) and is pushed upwards by the scattering force (d, e). Finally, it remains trapped at the upper cover slip (f) until the laser is turned off again.

5. Conclusion

We have fabricated photoresist microlenses with nearly ideal spherical shapes on top-emitting GaAs/AlGaAs VCSELs. The good output performance of the devices is not degraded by the lens, while the output beam is focussed to a beam waist of about $10\text{ }\mu\text{m}$ FWHM. With these devices, we have achieved elevation and trapping of $10\text{ }\mu\text{m}$ diameter polystyrene microspheres at output powers as small as 9 mW . Thus, the concept of VCSEL-based integrated optical traps is successfully demonstrated for the first time. By attaching the VCSELs directly to the sample stage and extending the concept to array configurations, miniaturised instruments for cell analysis and sorting appear to be within reach.

References

- [1] A. Ashkin, "Acceleration and trapping of particles by radiation pressure," *Phys. Rev. Lett.*, vol. 24, no. 4, pp. 156–159, 1970.
- [2] C.M. Creely, G. Volpe, G.P. Singh, M. Soler, and D.V. Petrov, "Raman imaging of floating cells," *Optics Express*, vol. 13, no. 16, pp. 6105–6110, 2005.
- [3] K. Ladavac, K. Kasza, and D.G. Grier, "Sorting mesoscopic objects with periodic potential landscapes: optical fractionation," *Phys. Rev. E*, vol. 70, pp. 010901-1–4, 2004.
- [4] A.L. Birkbeck, R.A. Flynn, M. Ozkan, D. Song, M. Gross, and S.C. Esener, "VCSEL arrays as micromanipulators in chip-based biosystems," *Biomedical Microdevices*, vol. 5, no. 1, pp. 47–54, 2003.
- [5] Y. Ogura, T. Beppu, F. Sumiyama, and J. Tanida, "Toward photonic computing: developing optical techniques for parallel manipulation of DNA," in *Photonics for Space Environments*, E.W. Taylor (Ed.), Proc. SPIE, vol. 5897, pp. 34–43, 2005.
- [6] F. Sumiyama, Y. Ogura, and J. Tanida, "Stacking and translation of microscopic particles by means of 2×2 beams emitted from a vertical-cavity surface-emitting laser array," *Appl. Phys. Lett.*, vol. 82, no. 18, pp. 2969–2971, 2003.
- [7] H.J. Unold, S.W.Z. Mahmoud, R. Jäger, M. Golling, M. Kicherer, F. Mederer, M.C. Riedl, T. Knödl, M. Miller, R. Michalzik, and K.J. Ebeling, "Single-mode VCSELs," in *Vertical-Cavity Surface-Emitting Lasers VI*, C. Lei, S.P. Kilcoyne (Eds.), Proc. SPIE, vol. 4649, pp. 218–229, 2002.